

RESEARCH ARTICLE | APRIL 26 2024

ExROPPP: Fast, accurate, and spin-pure calculation of the electronically excited states of organic hydrocarbon radicals

EP

Special Collection: [2024 JCP Emerging Investigators Special Collection](#)

James D. Green ; Timothy J. H. Hele  



J. Chem. Phys. 160, 164110 (2024)

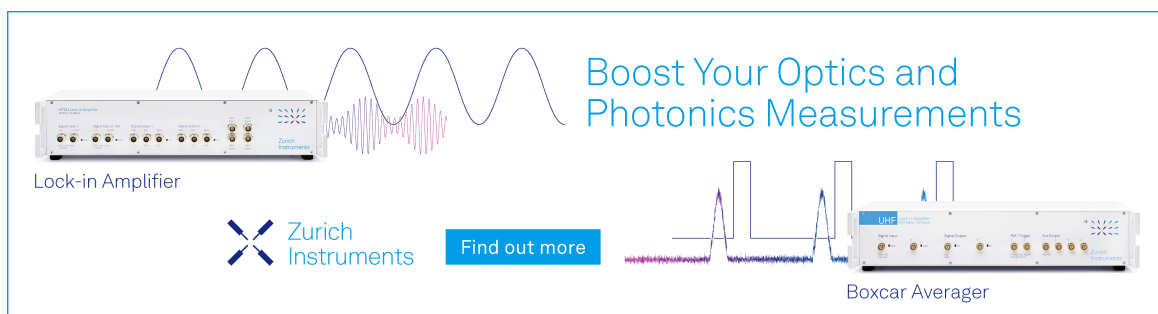
<https://doi.org/10.1063/5.0191373>



View
Online




Export
Citation



Boost Your Optics and Photonics Measurements

Lock-in Amplifier

 Zurich Instruments

[Find out more](#)

Boxcar Averager

ExROPPP: Fast, accurate, and spin-pure calculation of the electronically excited states of organic hydrocarbon radicals

Cite as: J. Chem. Phys. 160, 164110 (2024); doi: 10.1063/5.0191373

Submitted: 13 December 2023 • Accepted: 20 March 2024 •

Published Online: 26 April 2024



View Online



Export Citation



CrossMark

James D. Green  and Timothy J. H. Hele ^{a)} 

AFFILIATIONS

Department of Chemistry, Christopher Ingold Building, University College London, London WC1H 0AJ, United Kingdom

Note: This paper is part of the 2024 JCP Emerging Investigators Special Collection.

^{a)} Author to whom correspondence should be addressed: t.hele@ucl.ac.uk

ABSTRACT

Recent years have seen an explosion of interest in organic radicals due to their promise for highly efficient organic light-emitting diodes and molecular qubits. However, accurately and inexpensively computing their electronic structure has been challenging, especially for excited states, due to the spin-contamination problem. Furthermore, while alternancy or “pseudoparity” rules have guided the interpretation and prediction of the excited states of closed-shell hydrocarbons since the 1950s, similar general rules for hydrocarbon radicals have not to our knowledge been found yet. In this article, we present solutions to both of these challenges. First, we combine the extended configuration interaction singles method with Pariser–Parr–Pople (PPP) theory to obtain a method that we call ExROPPP (Extended Restricted Open-shell PPP) theory. We find that ExROPPP computes spin-pure excited states of hydrocarbon radicals with comparable accuracy to experiment as high-level general multi-configurational quasi-degenerate perturbation theory calculations but at a computational cost that is at least two orders of magnitude lower. We then use ExROPPP to derive widely applicable rules for the spectra of alternant hydrocarbon radicals, which are completely consistent with our computed results. These findings pave the way for highly accurate and efficient computation and prediction of the excited states of organic radicals.

© 2024 Author(s). All article content, except where otherwise noted, is licensed under a Creative Commons Attribution (CC BY) license (<http://creativecommons.org/licenses/by/4.0/>). <https://doi.org/10.1063/5.0191373>

I. INTRODUCTION

It was long thought that the search for stable emissive organic radicals was hopeless, as none were known experimentally.¹ However, since the discovery of stable, highly emissive organic radicals and the development of highly emissive radical organic light-emitting diodes (OLEDs), there has been an explosion of interest in the field.^{2–8} External quantum efficiencies in excess of 25% and internal quantum efficiencies of near unity³ for some radical-based devices have been reported. Although phosphorescent OLEDs based on molecules containing heavy elements and those based on organic closed-shell molecules that exhibit thermally activated delayed fluorescence also have high efficiencies, such figures are usually hard to achieve in conventional closed-shell OLEDs due to spin-statistics.^{9–15} Such high-performing OLEDs have potential applications in the next generation of lightweight and flexible displays and lighting.³ Moreover, radical-based devices can achieve

this intense emission in the near-infrared (NIR) region, a characteristic that is unusual for small molecules and highly desirable for the development of fluorescent probes and NIR sources for medical diagnostic applications.^{16–19} Emissive organic radicals have since been incorporated into emissive conjugated polymers,⁷ which opens up the possibility of having the efficiency and spectral benefits of a radical emitter with the processability advantages of conjugated polymers and also the possibility of semiconductivity.^{11,20} In addition, emissive organic radicals have potential applications as spin-optical interfaces in quantum information processing.²¹

While there has been considerable work done over the years to investigate the electronic structure of radicals, diradicals, and polyradicals,^{22–24} accurately computing their electronic structure remains challenging largely due to spin-contamination. The first problem is whether to use unrestricted or restricted orbitals as the most obvious choice that gives the most accurate energies and the best description of the ground state are unrestricted orbitals, but

using those results in spin-contamination. The second problem is the choice of determinants for the excited states as including all single-excitations in configuration interaction singles (CIS) results in spin-contaminated excited states, even when using a restricted basis.^{24–27} Furthermore, while general alternancy or pseudoparity rules have been known since the 1950s²⁸ to assign, predict, and interpret the spectra of closed-shell hydrocarbons, to the best of our knowledge, no such general rules exist for the excited states of hydrocarbon radicals.

In this article, focusing on organic radicals with a single unpaired electron (monoradicals), we give a detailed overview of some of the existing theories for radical electronic structure calculation, the challenges that arise when it comes to excited states of radicals, and how or if they can be overcome. We then expand on this previous work seeking to provide new insight into the properties of the excited electronic states of radicals.

One problem encountered in the calculation of the electronically excited states of radicals is that there is no ideal set of orbitals to choose from. Both the unrestricted Hartree–Fock (UHF) method²⁹ and the restricted open-shell Hartree–Fock (ROHF) method^{30–33} have their shortfalls. While UHF is often preferred as it gives lower, more accurate energies due to each of the electrons having different spatial orbitals, UHF states comprising a finite linear combination of UHF determinants are generally not eigenfunctions of the total spin operator \hat{S}^2 .³⁴ Although UHF (and unrestricted density functional theory) is a useful tool for calculating accurate ground state properties, and in many such cases the spin-contamination can be ignored,^{22,35–42} it can be problematic for excited states where spin-contamination is unavoidable and can lead to unphysical or uninterpretable results.^{22,24,27,43–45} Conversely, ROHF eliminates spin-contamination by construction for states where all unpaired electrons are of the same spin, including the ground state. Furthermore, it is possible to form spin-adapted ROHF configurations in a finite number of determinants for all other states.^{24,27,30–34,41} However, ROHF has its weaknesses, namely, that it gives less accurate energies than UHF and also the issue of orbital energies not being uniquely defined.^{46,47}

Although both UHF and ROHF clearly have their own limitations, for calculation of the photophysical properties of radicals, we believe that spin-purity must take precedence over a slight improvement in accuracy. However, using a restricted reference is not a sufficient criterion on its own for satisfying the spin-purity of the excited states, as it should be ensured that the correct linear combinations of determinants are chosen for states with more than one open-shell.

This brings us to the second major challenge in preserving the spin-purity of the excited states. In the case of closed-shell molecules, from the set of all single-excitations of α and β electrons, $|\Phi_i^{j'}\rangle$ and $|\Phi_i^{\bar{j}'}\rangle$, respectively, one can form a complete set of spin-adapted singlet $|\Psi_i^{j'}\rangle$ and triplet $|\Psi_i^{\bar{j}'}\rangle$ configurations or configuration state functions (CSFs) from a restricted determinant in configuration interaction singles (CIS). This is the simplest configuration interaction method and the formal starting point for many other more accurate methods.^{34,41,48} Usually, we are only interested in the singlet states with regard to absorption and emission as triplet states are formally dark. However, caution must be taken when choosing

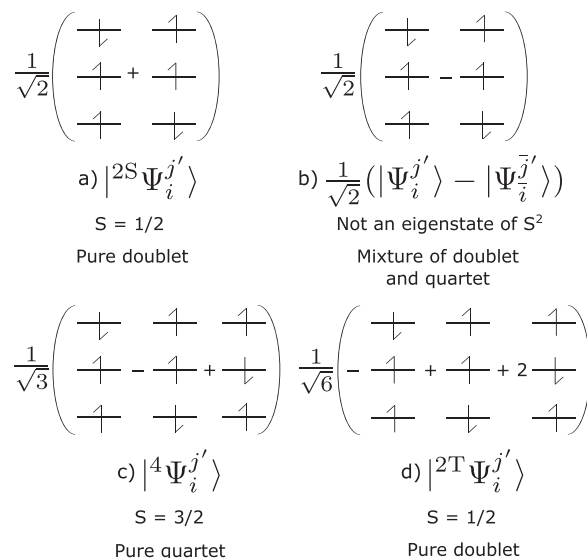


FIG. 1. Illustration of the problem of using only single excitations to describe the excited states of a doublet radical that consist of three open-shells. Four excited configurations are pictured: (a) the spin-pure singlet-coupled doublet (2S) state (“+” combination) formed of only single excitations, (b) the “−” combination of two single excitations that is spin-contaminated, (c) the spin-pure quartet state composed of single and double excitations, and (d) the spin-pure triplet-coupled doublet (2T) state composed of single and double excitations.

a basis for the excited states of radicals. First, if one were to use a basis of all single excitations, as in the closed-shell case, and form a complete set of states, this would, in general, result in spin-contamination. This is shown pictorially in Fig. 1 below and also presented numerically Table X, where we have presented the results of this approach for the benzyl radical. The general spin properties of closed-shell molecules and radicals are presented in Table I.

One solution to the spin-contamination problem in radical CIS is to restrict the basis of single excitations to only include those that are pure doublets, which are those with only one open-shell, in which case the resulting states would also be pure doublets. Alternatively, one could go a step further and also add in some spin-adapted doublet states for those configurations containing three open-shells;⁴⁹ however, neither method captures quartet states. Furthermore, some excited doublet states with three open-shells are also not captured by these methods, which, despite being dark, could affect the spectrum. This problem is solved if one also includes a certain type of double excitations in the basis, as shown in previous literature, and in this case a complete set of spin-pure doublet and quartet states can be constructed on the same theoretical footing in a similar manner to closed-shell CIS.^{24,25} This formulation of open-shell CI, which is discussed further in Sec. II is sometimes referred to as extended CIS or XCIS.²⁵ This is different to CISD where all double excitations are included and which would not, in general, be spin-pure for radicals. In addition, XCIS has the same scaling as CIS, where the number of determinants scales with $\mathcal{O}(N_{\text{occ}}N_{\text{vir}})$, whereas CISD scales with $\mathcal{O}(N_{\text{occ}}^2N_{\text{vir}}^2)$, where N_{occ} is the number of occupied

TABLE I. Comparison of the general spin properties of the singly excited electronic states for closed-shell molecules and radicals.

Property	Closed-shell	Radical
Ground state multiplicity	Singlet	Doublet
Determinant	RHF	ROHF or UHF
Spin-multiplicity of single-excitations	$ \Psi_i^{j'}\rangle + \Psi_i^{\bar{j}'}\rangle$ is singlet. $ \Psi_i^{j'}\rangle - \Psi_i^{\bar{j}'}\rangle$ is triplet.	$ \Psi_i^0\rangle, \Psi_0^{j'}\rangle, \Psi_i^{j'}\rangle + \Psi_i^{\bar{j}'}\rangle$ are doublets. $ \Psi_i^{j'}\rangle - \Psi_i^{\bar{j}'}\rangle$ contaminated.
Usual multiplicity of lowest excited state	Triplet	Doublet
Spin restriction alone sufficient for spin-purity?	Yes	No

orbitals and N_{vir} is the number of virtual (unoccupied) orbitals in the ground state.

We must stress here that there are many other existing methods to obtain accurate, spin-pure excited states of radicals, such as the multiconfigurational SCF (MCSCF) method, multiconfigurational second-order perturbation theory, such as CASPT2 and general multi-configurational quasi-degenerate perturbation theory (GMC-QDPT) mentioned later, full-CI (FCI), and coupled-cluster (CC) theory.^{34,50–53} These methods achieve spin-pure results for radicals by using a restricted open-shell reference and by either including all possible configurations (within a given active space in MCSCF and CASPT2/GMCQDPT) or including fewer than all possible configurations and employing spin-adaptation techniques.^{54–56} When used correctly, these methods can give accurate results,⁵⁷ although for very accurate excitation energies, one must also include nuclear quantum effects.⁵⁸ However, these calculations are computationally expensive, with their computational cost increasing by many orders of magnitude with increasing molecular size, and also are by no means black-box methods, requiring chemical intuition and experience to be accurately utilized.³⁴ One potential avenue is to decrease the computational cost of such methods by, for example, combining MCSCF or FCI with quantum Monte Carlo; however, discussions on this topic are beyond the scope of this article.^{59,60} On the other hand, time-dependent density functional theory (TD-DFT) allows for the rapid calculation of electronic excited state spectra, which does not require any non-trivial input from the user and has become a popular method for the simulation of UV-visible spectra.^{61,62} However, TD-DFT has several drawbacks, namely, that: (a) its results can vary significantly depending on the chosen functional,^{61,62} (b) it is inaccurate at describing long-range phenomena, such as charge-transfer without the use of specifically tailored long-range functionals,^{63–66} and (c) it does not typically give spin-pure states, as an unrestricted version of the Kohn–Sham equations is often preferred in favor of more accurate energies, and even if a restricted open-shell reference is used, conventional TD-DFT does not form spin-adapted excited states.^{44,45} A spin-adapted version of TD-DFT for radicals has recently been developed, called X-TDDFT, which is clearly a faster alternative to the more expensive MCSCF/CASPT2/GMC-QDPT/FCI/CC methods.⁴⁵ However, X-TDDFT is by no means theoretically straightforward since the double excitations it requires are not compatible with

conventional TD-DFT so a work-around using spin-flip single excitations and reference states with different values of M_s needs to be implemented. Finally, although TD-DFT is faster than the post-Hartree–Fock methods mentioned above, it still becomes unfeasibly expensive for large numbers of calculations, and there is a growing need for ever faster property determination methods for high-throughput virtual screening of molecular candidates, artificial intelligence (AI) algorithm search methods, and for property determination of large molecules.^{67–69}

This brings us to two key aims, which we will address in this paper.

A. An inexpensive method for screening radicals

What is the simplest and least computationally expensive method that can calculate spin-pure doublet and quartet states of radicals with reasonable accuracy?

B. Design rules for emissive radicals based on alternant hydrocarbons

A general set of rules for the interaction of the excited states of radicals would allow for a better understanding of their UV-visible spectra, guiding the assignment of bands and allowing us to predict the effect of structural variations on their spectra. Considering that many emissive radicals are (non-alternant) derivatives of alternant hydrocarbons, such as the triphenylmethyl radical,^{2–7} a good starting point would be to deduce such design rules for alternant hydrocarbon radicals.

The article is structured as follows: first, in Sec. II, we define the key theoretical concepts that will inform the discussion of our methodology. Here, we discuss the XCIS method for doublet radicals,^{24,25} a restricted open-shell method for the molecular orbitals,²⁴ Pariser–Parr–Pople theory and its approximations,^{28,70–73} and also give a brief overview of the theories relating to alternant hydrocarbons.^{28,72,74} In Sec. III, we show how the XCIS and PPP theory with a restricted open-shell determinant can be combined and implemented in a method that we call Extended Restricted Open-shell PPP (ExROPPP) theory, for the rapid calculation of spin-pure excited states of radicals, which is not limited to just alternant hydrocarbons. The numerical results of computations with ExROPPP are presented in Sec. IV A, where the method is benchmarked

against the highly accurate multiconfigurational perturbation theory method GMC-QDPT and experimental data, where ExROPPP is seen to have a similar accuracy to GMC-QDPT. Finally, in Sec. IV B, we then apply the algebra of XCIS to alternant hydrocarbons, and by making a small number of approximations, we derive rules for the interaction of excited states of alternant hydrocarbon radicals similar to those derived previously for closed-shell molecules.²⁸ We believe that these rules may aid with the assignment of bands in the UV-visible spectra of radicals and also guide the design of emissive radicals.

II. BACKGROUND THEORY

Here, we discuss the XCIS method for the excited states of radicals,^{24,25} the restricted open-shell method of Longuet-Higgins and Pople,²⁴ which allows us to obtain self-consistent molecular orbitals for a system with one unpaired electron in its ground state; the various approximations of the Pariser-Parr-Pople (PPP) theory;^{28,70–73} and finally, the theories of Coulson, Rushbrooke, Pople and Pariser, which apply alternant hydrocarbons that we will call upon to derive the alternancy rules for radicals.^{28,72,74}

A. From CIS to XCIS

We start by discussing the description of the ground state of the radical. Restricted orbitals are chosen where k doubly occupied closed-shells and one singly occupied open-shell make up the ground state, which is a pure doublet with $S = M_S = 1/2$. We label the orbitals, choosing 0 to be the singly occupied molecular orbital (SOMO), and successively number the doubly occupied orbitals in order of descending energy starting from 1 (the HOMO) and the vacant orbitals in order of ascending energy with primes starting from 1' (the LUMO). We choose this notation as it is the same as that used by Pariser²⁸ and in Ref. 27. We now discuss the excited configurations. Single excitations from the ground state $|^2\Psi_0\rangle$ give rise to the following configurations: $|^2\Psi_i^0\rangle$, $|^2\Psi_0^{j'}\rangle$, $|\Psi_i^{j'}\rangle$, and $|\Psi_i^{j'}\rangle$ (see Fig. 1 in the supplementary material for a comprehensive molecular orbital diagram).

As we are concerned with finding those states that are eigenstates of the total spin operator \hat{S}^2 , we shall ascertain the effect of \hat{S}^2 on the above-mentioned configurations. The states $|^2\Psi_0\rangle$, $|^2\Psi_i^0\rangle$, and $|^2\Psi_0^{j'}\rangle$ are eigenstates of \hat{S}^2 , where $S = 1/2$ —these configurations are pure doublet states. This is to be expected as they have only one open-shell. On the other hand, those configurations that have three open-shells, $|\Psi_i^{j'}\rangle$ and $|\Psi_i^{j'}\rangle$, are not eigenstates of \hat{S}^2 and are mixtures of doublet and quartet states. Naturally, we can make two orthonormal linear combinations of $|\Psi_i^{j'}\rangle$ and $|\Psi_i^{j'}\rangle$,

$$|^2S\Psi_i^{j'}\rangle = \frac{1}{\sqrt{2}}\left(|\Psi_i^{j'}\rangle + |\Psi_i^{j'}\rangle\right), \quad (1a)$$

$$|^2Q\Psi_i^{j'}\rangle = \frac{1}{\sqrt{2}}\left(|\Psi_i^{j'}\rangle - |\Psi_i^{j'}\rangle\right), \quad (1b)$$

to see if we can construct two spin-adapted states. We find that the “+” combination is a pure doublet with $S = 1/2$; however, the “−” combination is not an eigenstate of \hat{S}^2 . Then, it is clearly impossible

to construct a spin-pure basis for doublet and quartet excited states of a radical from just single excitations from the ground state.

As previous literature has shown, one must, therefore, go to higher-order excitations to attempt to satisfy spin-purity while calculating doublet and quartet states on the same theoretical footing.^{24,25} Double excitations of the type $|\Psi_{i0}^{0j'}\rangle$ were suggested as, along with the single-excitations $|\Psi_i^{j'}\rangle$ and $|\Psi_i^{j'}\rangle$, they complete all permutations of three open-shells in orbitals i , 0, and j' with $M_S = 1/2$.

One can construct the matrix representation of \hat{S}^2 in the basis of the following three excitations: $|\Psi_i^{j'}\rangle$, $|\Psi_i^{j'}\rangle$, and $|\Psi_{i0}^{0j'}\rangle$,

$$S^2 = \begin{pmatrix} 7/4 & -1 & 1 \\ -1 & 7/4 & -1 \\ 1 & -1 & 7/4 \end{pmatrix}, \quad (2)$$

which has eigenvalues of 3/4 twice and 15/4, corresponding to two doublet eigenstates and one quartet eigenstate,

$$|^2S\Psi_i^{j'}\rangle = \frac{1}{\sqrt{2}}\left(|\Psi_i^{j'}\rangle + |\Psi_i^{j'}\rangle\right), \quad (3a)$$

$$|^2T\Psi_i^{j'}\rangle = \frac{1}{\sqrt{6}}\left(-|\Psi_i^{j'}\rangle + |\Psi_i^{j'}\rangle + 2|\Psi_{i0}^{0j'}\rangle\right), \quad (3b)$$

$$|^4\Psi_i^{j'}\rangle = \frac{1}{\sqrt{3}}\left(|\Psi_i^{j'}\rangle - |\Psi_i^{j'}\rangle + |\Psi_{i0}^{0j'}\rangle\right). \quad (3c)$$

These three states, along with $|^2\Psi_0\rangle$, $|^2\Psi_i^0\rangle$, and $|^2\Psi_0^{j'}\rangle$, constitute a basis for the spin-pure excited doublet and quartet states of a radical and will be the starting point for our methodology.^{24,25,27} Here, we note that while the quartet eigenstate $|^4\Psi_i^{j'}\rangle$ is uniquely defined, the two doublet eigenstates are not, since they are spin degenerate and can be mixed. We label the first doublet state [Eq. (3a)] 2S as it can have a nonvanishing dipole moment from the ground state^{24,27} and is sometimes referred to as “singlet-coupled,”⁷⁵ and we refer to the second doublet state [Eq. (3b)] as 2T as it is always completely dark and is sometimes referred to as “triplet-coupled.”⁷⁵

B. The restricted open-shell method for the orbitals

While there are many variations of restricted open-shell methods to choose from, we elect to use the method of Longuet-Higgins and Pople.²⁴ In this method, the ground state orbitals are solved variationally as per the usual HF method, but in this case, minimizing the ground state energy with respect to mixing of small amounts of single excitations $|\Psi_i^0\rangle$, $|^2\Psi_0^{j'}\rangle$, and $|^2S\Psi_i^{j'}\rangle$ into the ground state.

They propose a single Fock operator for both closed-shell and open-shell spin-orbitals,

$$\langle\psi_p|\hat{H}|\psi_q\rangle = F_{pq} = h_{pq} + \sum_{l=1}^k [2(pq|ll) - (pl|lq)] + \frac{1}{2}[2(pq|00) - (p0|0q)]. \quad (4)$$

In this method, the ground state mixing of the configuration $|\Psi_i^{2s}\rangle$ is exactly zero; however, the ground state mixing of the configurations $|\Psi_i^0\rangle$ and $|\Psi_i^1\rangle$ is *almost* but not exactly zero (see the supplementary material for further details). Therefore, Brillouin's theorem is *almost* but not completely satisfied. As a note here, there are other restricted open-shell approaches for the orbitals that are more general in that they can be applied to systems with more than one open-shell in the ground state, and they also satisfy Brillouin's theorem exactly.^{30–33} However, these more general methods involve partitioning the set of orbitals into interacting subspaces for doubly occupied, partially occupied, and vacant orbitals each with their respective Fock operators, requiring the use of Lagrange multipliers to solve the coupled Roothaan equations while maintaining spin-restriction.^{30–33} While this ensures Brillouin's theorem is satisfied exactly, these methods are complicated to implement, and therefore, we elect to use the approximate method of Longuet-Higgins and Pople for systems with a single open-shell doublet ground state, despite it only approximately satisfying Brillouin's theorem, as it is theoretically simpler and involves only diagonalizing a single Fock matrix for all orbitals. As we shall see later, this simple form of the Fock operator also allows the derivation of elegant rules for the spectra of alternant hydrocarbon radicals.

C. Pariser-Parr-Pople theory

Thus far, in our discussion of the method to obtain the molecular orbitals, we have assumed an arbitrary basis of atomic orbitals and have not detailed the method to be used to obtain the one-electron (core) integrals $h_{\mu\nu}$ and two-electron integrals $(\mu\nu|\rho\sigma)$ needed to form the Fock matrix. We could elect to use Gaussian orbitals and compute the integrals for the set of all atomic orbitals exactly; however, this comes at a computational expense that we aim to minimize. We, therefore, call upon Pariser-Parr-Pople (PPP) theory^{28,70–73} as it is arguably the simplest and least computationally expensive method known to accurately reproduce the excited state spectra of π -conjugated closed-shell molecules,^{76,77} and we will see that it performs similarly well for π -conjugated organic radicals when using restricted orbitals and coupled with XCIS in a method that we call ExROPPP. Moreover, due to the approximations within PPP theory, many integrals vanish and many different integrals become equivalent, simplifying the form of the Hamiltonian and other electron operators. Therefore, applying the approximations of PPP theory to the Hamiltonian and dipole moment operators within XCIS allows us to derive alternancy rules.

PPP theory is a semiempirical method for the electronic structure calculation of conjugated π systems. The π system is treated using an implicit basis of p orbitals centered on the atomic nuclei, where neighboring p orbitals interact via a Hückel β (resonance integral) term. The σ system is treated as core-like and only interacts with the π system through a Hückel α (core integral) term, which also accounts for nuclear charge.

In PPP theory, the neglect of differential overlap (NDO) approximation is applied, where the overlap integral between any two atomic orbitals is equal to the Kronecker delta function of the two orbitals, $\langle\phi_\mu|\phi_\nu\rangle = \delta_{\mu\nu}$. First, this means that the Roothaan equations simplify to $\mathbf{FC} = \mathbf{CE}$, where \mathbf{E} is a diagonal matrix of

orbital energies $\{\epsilon_p\}$. The second implication of NDO is that the expressions for the two-electron integrals are greatly simplified, as those integrals that depend on the overlap of two p orbitals on different atoms are neglected. Therefore, the two-electron integrals take the form,

$$(\mu\nu|\rho\sigma) = (\mu\mu|\rho\rho)\delta_{\mu\nu}\delta_{\rho\sigma} = \gamma_{\mu\rho}\delta_{\mu\nu}\delta_{\rho\sigma}, \quad (5)$$

where $\gamma_{\mu\rho}$ is a function of the distance between the two atomic centers.²⁷

D. Alternant hydrocarbon radicals

Alternant hydrocarbons are conjugated hydrocarbons whose atoms can be divided into two sets, often referred to as *starred* and *unstarred*, where no two atoms of the same set may be directly bonded. This structural symmetry results in underlying symmetries in the energies and coefficients of pairs of orbitals and degeneracy of pairs of single-excitations. This pairing theorem was first proven by Coulson and Rushbrooke for closed-shell systems, where it was shown to hold under the approximations of neglect of differential overlap (NDO) and resonance interaction only between nearest neighboring atoms, such approximations being present in Pariser-Parr-Pople theory (see Sec. II C).⁷⁴ Subsequently, the Coulson-Rushbrooke pairing theorem was also shown to hold for odd alternant hydrocarbon radicals.^{24,78} This symmetry of alternant hydrocarbons is sometimes referred to as pseudoparity, particle-hole symmetry, or the Coulson-Rushbrooke-Longuet-Higgins theorem.^{79–81}

1. Orbital energy symmetry

According to the theorem, for every bonding orbital, there exists an antibonding orbital with an equal and opposite energy relative to the energy of a non-interacting atomic orbital. In the case of monoradicals, the SOMO has a non-bonding character and its energy is the same as that of a non-interacting orbital, and all *other* orbitals can be grouped into bonding and antibonding pairs, which are equally spaced in energy about the SOMO, $(\epsilon_i + \epsilon_r)/2 = (F_{i,i} + F_{r,r})/2 = \epsilon_0 = F_{0,0}$.

2. Orbital coefficient symmetry

In alternant hydrocarbon radicals, the SOMO has amplitude on only the *starred* atoms, and for every Coulson-Rushbrooke orbital pair, the orbital coefficients in bonding and antibonding pairs (i) are equal in magnitude and (ii) have equal signs on the *starred* atoms and opposite signs on the *un-starred* atoms. In the convention followed in this paper, the number of *starred* atoms is one greater than the number of *unstarred* atoms for odd alternant hydrocarbon radicals. The following is then true for two electron integrals for alternant hydrocarbon radicals: $(ij|kl) = (ij|k'l') = (i'j'|kl) = (i'j'|k'l')$, and $(i0|jk) = (i'0|j'k)$. The latter relation is a special case of the first two because the SOMO is unchanged by changing the signs of the *un-starred* atoms, i.e., $\psi_0 = \psi_{0'}$. Similar identities also exist for dipole moments, $\mu_{ij} = \mu_{i'j'}$, $\mu_{ij'} = \mu_{i'j}$, and $\mu_{i0} = \mu_{i'0}$, where we use the standard definition of the dipole moment in atomic units, $\mu_{ij} = \langle i|\hat{\mu}|j\rangle = -\langle i|\mathbf{r}|j\rangle$.

3. Degeneracy of the excited states with a single open-shell

These symmetry relations result in degeneracies in pairs of excitations, even when two electron terms are taken into account within the regime of the above-mentioned approximations. The excitations $|^2\Psi_i^0\rangle$ and $|^2\Psi_i^{\prime}\rangle$ are degenerate for the corresponding pairs of bonding and antibonding orbitals, ψ_i and ψ_i^{\prime} . They can be factored into two-determinant linear combinations with a “+” or “−” sign, as shown in the following equation:^{24,27}

$$|^2\Psi_{0i}^{\pm}\rangle = \frac{1}{\sqrt{2}}\left(|^2\Psi_i^0\rangle \pm |^2\Psi_i^{\prime}\rangle\right). \quad (6)$$

III. METHODOLOGY

We introduce a novel method, which we call the ExROPPP (Extended Restricted Open-shell Pariser–Parr–Pople) theory for the rapid and accurate simulation of spin-pure excited states of organic π -conjugated radicals. This method marries the idea of XCIS^{24,25} with PPP theory^{28,70–73} using the restricted open-shell method of Ref. 24. We implement the equations in Secs. II B and II C in an in-house code, using the same parameters as those used previously for closed-shell molecules,⁶⁹ to form the restricted open-shell Fock matrix in PPP theory and to subsequently obtain the optimized molecular orbital coefficients and orbital energies by iteratively solving the Roothaan equations until convergence of the total energy. The essential equations of XCIS discussed in Sec. II A (see $\mathbf{H}_{\text{XCIS}}^s$, $\mathbf{H}_{\text{XCIS}}^x$, $\mathbf{M}_{\text{XCIS}}^x$, and $\mathbf{M}_{\text{XCIS}}^s$ in the supplementary material, Tables IX, X, XIII, and XIV) are then implemented to form and diagonalize the XCIS Hamiltonian to give the energies and expansion coefficients of the XCIS excited states and to compute their dipole moments and oscillator strengths for the plotting of linear absorption spectra. This method was benchmarked on a series of alternant hydrocarbon radicals, and the results of these computations are given in Sec. IV. However, we must stress that this method is not limited to just alternant hydrocarbon radicals but can be applied to any radical with one unpaired electron in its ground state.

IV. RESULTS

In this section, we now present the central results of this paper. First, we present the results of numerical calculations on a range of alternant hydrocarbon radicals with our new method, ExROPPP, where ExROPPP is shown to be accurate in comparison to the experimental data and higher-level methods, spin-pure and computationally inexpensive. Second, we reveal the simple and elegant rules of interaction between the excited states of alternant hydrocarbon radicals, similar to those found by Pariser for closed-shell molecules,²⁸ which we believe could aid the design of radicals.

A. Numerical results from ExROPPP on alternant hydrocarbon radicals

Here, we present the results of our new method, ExROPPP, benchmarked against experimental data and the results of calculations with general multi-configurational quasi-degenerate

perturbation theory (GMC-QDPT), an accurate post-Hartree–Fock method for calculating excited states. The UV–visible vertical absorption spectra of a series of odd alternant hydrocarbon radicals shown in Fig. 2 were simulated using the ExROPPP method described in Sec. III, and these results were also compared to the results of calculations using GMC-QDPT and experimental spectroscopic data in the literature, where available. We must stress here that we choose to use alternant hydrocarbons to demonstrate the utility of ExROPPP, despite the fact ExROPPP is not limited to just alternant hydrocarbons, as they are generally stable, and thus, there is a large amount of experimental spectroscopic data available for them in the literature. In addition, since many emissive radicals are non-alternant derivatives of alternant hydrocarbons, the results of these computations are still of relevance to the design of emissive radicals. The ExROPPP and GMC-QDPT simulated spectra of the radicals are presented together in Figs. 3–5, and their spectroscopically observed states computed by the two theoretical methods compared to the experimental data are presented in Tables II–VIII, with further detail presented in Tables I–VII of the supplementary material. The results of the two theoretical methods are generally consistent with each other and closely reproduce the experimental excitation energies.

We now consider the accuracy, speed, and spin purity of ExROPPP.

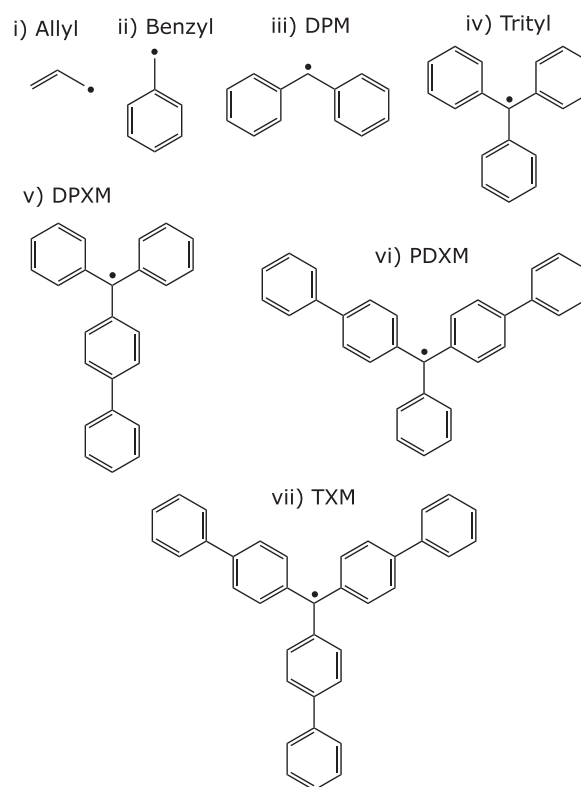


FIG. 2. Odd alternant hydrocarbons considered in this paper. The abbreviations were used for the following radicals: DPM—diphenylmethyl, DPXM—diphenyl-p-xenylmethyl, PDXM—phenyl-di-p-xenylmethyl, and TXM—tri-p-xenylmethyl.

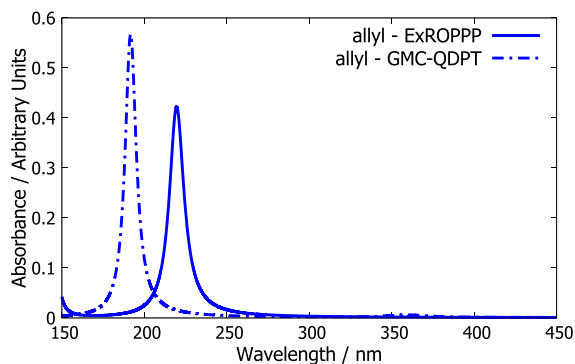


FIG. 3. UV-visible vertical absorption spectra of the allyl radical simulated by ExROPPP (solid blue) and GMC-QDPT (the blue dotted-dashed line).

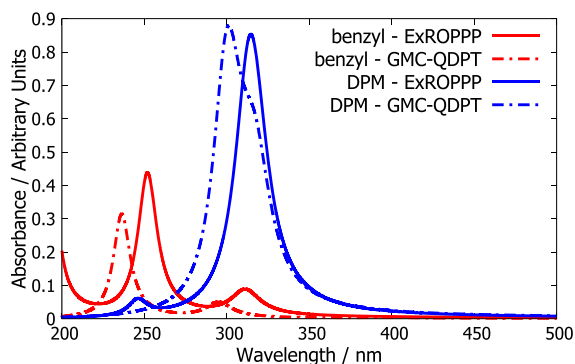


FIG. 4. UV-visible vertical absorption spectra of benzyl (red) and diphenylmethyl (blue) radicals simulated by ExROPPP (solid lines) and GMC-QDPT (the dotted-dashed lines).

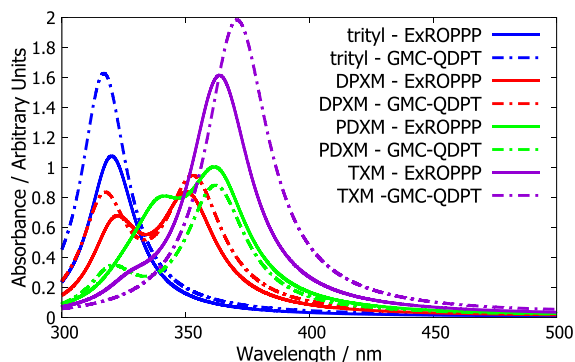


FIG. 5. UV-visible vertical absorption spectra of the trityl radical and its derivatives, DPXM, PDXM, and TXM, simulated by ExROPPP (solid lines) and GMC-QDPT (dotted-dashed lines), showing good agreement between the two methods.

1. Accuracy

a. The allyl, benzyl, and diphenylmethyl radicals. The ExROPPP and GMC-QDPT simulated spectra for these radicals are shown in Fig. 3 and 4, and their spectroscopic data are presented

TABLE II. Excitation energies of the allyl radical calculated by ExROPPP and GMC-QDPT compared to the experimental data.⁸²

State	E_{ExROPPP} (eV)	$E_{\text{GMC-QDPT}}$ (eV)	$E_{\text{exp.}}$ (eV)
1^2B_2	3.05	3.45	3.07
2^2B_2	5.65	6.47	5.00

TABLE III. Excitation energies of the benzyl radical calculated by ExROPPP and GMC-QDPT compared to the experimental data.⁸⁶

State	E_{ExROPPP} (eV)	$E_{\text{GMC-QDPT}}$ (eV)	$E_{\text{exp.}}$ (eV)
1^2A_2	2.89	3.05	2.76
2^2A_2	3.98	4.20	4.00
4^2B_2	4.92	5.25	4.77

TABLE IV. Excitation energies of diphenylmethyl radical calculated by ExROPPP and GMC-QDPT compared to the experimental data.⁸⁷

State	E_{ExROPPP} (eV)	$E_{\text{GMC-QDPT}}$ (eV)	$E_{\text{exp.}}$ (eV)
1^2A	2.64	2.56	2.37
4^2A	3.95	4.13	3.69

TABLE V. Excitation energies of the trityl radical calculated by ExROPPP and GMC-QDPT compared to the experimental data.⁹⁰

State	E_{ExROPPP} (eV)	$E_{\text{GMC-QDPT}}$ (eV)	$E_{\text{exp.}}$ (eV)
1^2E	2.74	2.63	2.41
2^2E	3.88	3.91	3.60

TABLE VI. Excitation energies of the DPXM radical calculated by ExROPPP and GMC-QDPT compared to the experimental data.⁹⁰

State	E_{ExROPPP} (eV)	$E_{\text{GMC-QDPT}}$ (eV)	$E_{\text{exp.}}$ (eV)
2^2B	2.56	2.40	2.07
3^2B	3.53	3.51	3.31
2^2A	3.86	3.91	3.60

TABLE VII. Excitation energies of the phenyl-di-p-xenylmethyl (PDXM) radical calculated by ExROPPP and GMC-QDPT compared to the experimental data.⁹⁰

State	E_{ExROPPP} (eV)	$E_{\text{GMC-QDPT}}$ (eV)	$E_{\text{exp.}}$ (eV)
1^2A	2.51	2.33	2.03
2^2A	3.42	3.42	3.03
3^2B	3.66	3.87	3.45

TABLE VIII. Excitation energies of the tri-*p*-xenylmethyl (TXM) radical calculated by ExROPPP and GMC-QDPT compared to the experimental data.⁹⁰

State	E_{ExROPPP} (eV)	$E_{\text{GMC-QDPT}}$ (eV)	$E_{\text{exp.}}$ (eV)
1^2E	2.52	2.30	2.03
2^2E	3.41	3.34	2.95

in Tables II–IV. The energies and relative intensities are generally consistent between the two theoretical methods and with the experimental data.

For the allyl radical, in the C_{2v} point group, the 1^2B_2 state (D_1) is composed of $|\Psi_{01}^- \rangle$ in both GMC-QDPT and ExROPPP and appears at 3.07 eV (404 nm) in the experiment⁸² and at 3.45 eV (360 nm) and 3.05 eV (407 nm) in GMC-QDPT and ExROPPP calculations, respectively, showing a good agreement, especially for ExROPPP. The experimental intensity of the 1^2B_2 state is known to be very weak in other studies,^{83,84} which is in agreement with the low oscillator strengths computed by GMC-QDPT and ExROPPP of 0.005 and 0, respectively. The 2^2B_2 state, $|\Psi_{01}^+ \rangle$ in GMC-QDPT and ExROPPP, appears at 5.00 eV (248 nm) in the experiment⁸² and 6.47 eV (192 nm) and 5.65 eV (220 nm) in GMC-QDPT and ExROPPP, respectively, showing a close agreement. 2^2B_2 is observed as a bright absorption in another study,⁸⁵ which is in agreement with GMC-QDPT and ExROPPP with oscillator strengths of 0.567 and 0.422, respectively.

The weak 1^2A_2 state (D_1) of the benzyl radical is seen around 2.76 eV (450 nm) in the experimental spectrum.⁸⁶ The 1^2A_2 state is predicted to be at 3.05 eV (407 nm) in GMC-QDPT and 2.89 eV (430 nm) in ExROPPP and similar to the allyl radical is predicted to be completely dark by ExROPPP (composed of $|\Psi_{01}^- \rangle$), with a very small oscillator strength predicted by GMC-QDPT. The 3^2B_2 state ($|\Psi_{02}^- \rangle$ in ExROPPP), which appears at 4.99 eV (248 nm) with $f \approx 0$ in GMC-QDPT and 4.50 eV (275 nm) with $f = 0$ in ExROPPP, is not seen in the experiment likely due to it having a vanishingly small intensity. The two bright states of the benzyl radical, 2^2A_2 and 4^2B_2 , which are composed of $|\Psi_{01}^+ \rangle$ and $|\Psi_{02}^+ \rangle$, respectively, in ExROPPP are seen in the experimental spectrum at 4.00 eV (310 nm) and 4.77 eV (260 nm), respectively.⁸⁶ These states are also well captured by GMC-QDPT [2^2A_2 at 4.20 eV (295 nm) and 4^2B_2 at 5.25 eV (236 nm)] and ExROPPP [2^2A_2 at 3.98 eV (311 nm) and 4^2B_2 at 4.92 eV (252 nm)] with a particularly good agreement in ExROPPP. The relative intensities of these transitions are also in agreement between the two theoretical methods, with the 4^2B_2 state predicted to be brighter than the 2^2A_2 by GMC-QDPT and ExROPPP, which is also consistent with the experimental spectrum.⁸⁶ While the agreement between ExROPPP and the experiment is slightly better for the bright states than the dark states, the overall accuracy of ExROPPP for the benzyl radical is as good as, if not better, than GMC-QDPT.

In the GMC-QDPT calculations, the orbitals 1 ($2b_2$) and 2 ($1a_2$) are swapped in the energetic order compared to ExROPPP, and the excited states seem to be composed of different excitations; however, on swapping the orbital indices 1 and 2 in the GMC-QDPT excitations, the states are the same as those in ExROPPP. To avoid confusion, we have omitted the compositions of the GMC-QDPT

states here and these results are given in the supplementary material.

The results for the benzyl radical are also supported by early theoretical results.^{88,89} In particular, Ref. 88 shows the same energy ordering and relative intensities of the excited states for the benzyl radical: 1^2A_2 (weak absorption), 2^2B_2 (weak absorption), 2^2A_2 (strong absorption), and 3^2B_2 (strong absorption, corresponds to 4^2B_2 in ExROPPP/GMC-QDPT). Ref. 88 only considered the first two orbitals above and below the SOMO in the benzyl radical, derived from the splitting of the 1^2E and 2^2E levels in benzene, not accounting for the extra dark state 3^2B_2 in ExROPPP, which involves orbitals 3 and 3' in the benzyl radical so the energetic ordering in both methods is essentially the same for the states captured by both.

For DPM, which belongs to the C_2 point group, the 1^2A state (D_1) appears at 2.37 eV (523 nm) in the experiment⁸⁷ and at 2.56 eV (485 nm) and 2.64 eV (470 nm) in GMC-QDPT and ExROPPP, respectively, and is primarily composed of $|\Psi_{01}^- \rangle$ in ExROPPP. This state has a weak absorption ($370 \text{ dm}^3 \text{ mol}^{-1} \text{ cm}^{-1}$)⁸⁷ in the experiment and is dark in GMC-QDPT and ExROPPP. The bright 4^2A state is seen at 3.69 eV (336 nm) in the experiment,⁸⁷ and its energy is well reproduced by GMC-QDPT and ExROPPP with values of 4.13 eV (300 nm) and 3.95 eV (314 nm), respectively, and is composed of $|\Psi_{01}^+ \rangle$ in ExROPPP. It has a high measured intensity of $31\,000 \text{ dm}^3 \text{ mol}^{-1} \text{ cm}^{-1}$, which is in agreement with the large oscillator strengths calculated by GMC-QDPT and ExROPPP of 0.714 and 0.781, respectively. Similarly as for the benzyl radical, the ExROPPP calculated energy of the bright state is in closer agreement with the experiment than with the dark (D_1) state. The energetic ordering of the doublet states in DPM is not the same in ExROPPP and GMC-QDPT due to near degeneracies and a high density of states at low energy.

b. The triphenylmethyl radical and its p-xenyl derivatives. The experimental UV–visible absorption spectra of the trityl (triphenylmethyl) radical and its *p*-xenyl derivatives, di-phenyl-*p*-xenylmethyl (DPXM), phenyl-di-*p*-xenylmethyl (PDXM), and tri-*p*-xenylmethyl (TXM) contain one or two intense absorption bands depending on the molecule's point symmetry and are seen at around 300–500 nm. They also have one or two very weak bands in the region of 500–700 nm in the visible spectrum.⁹⁰ Trityl and TXM, in the D_3 point group, both have a single intense near-UV band owing to the 2^2E state, which is mainly composed of the $|\Psi_{01}^+ \rangle$ and $|\Psi_{02}^+ \rangle$ states (excitations between the SOMO and the doubly degenerate HOMO/LUMO) as seen in GMC-QDPT and ExROPPP calculations. DPXM and PDXM, both of which belong to the C_2 group, have two intense bands owing to the $|\Psi_{01}^+ \rangle$ and $|\Psi_{02}^+ \rangle$ states due to the removal of their degeneracy in descending order from D_3 to C_2 symmetry, with one of them having the irreducible representation A and the other B (the assignment of A or B to the excitations above differs between the two radicals). The ExROPPP and GMC-QDPT simulated spectra of these four radicals are shown in Fig. 5 and their spectroscopic data are presented in Tables V–VIII (and in more detail in Tables IV–VII in the supplementary material).

There is a good agreement between ExROPPP and the experimental data for these four radicals, which is better for the bright UV “+” states as opposed to the dark lowest energy excited “–” states

in the visible, which are completely dark in ExROPPP (due to the radicals all being alternant) and only have a very small extinction coefficient in the experimental spectra. For the bright transitions, the ExROPPP values are within 0.28 eV (25 nm) of the experimental value for trityl, 0.26 eV (24 nm) for DPXM, 0.39 eV (48 nm) for PDXM, and 0.46 eV (56 nm) for TXM. It is suggested by Ref. 90 that the lowest excited state of the trityl and TXM radicals is of A_1 symmetry from analysis of the fluorescence polarization data; however, we believe this not to be the case as this lowest excited state of the trityl radical has been shown to be a doubly degenerate E state in a later publication⁹¹ and in our results. The results of GMC-QDPT calculations for these radicals are also in good agreement with ExROPPP, and the relative energy ordering of the doublet states is the same in both methods.

The excitation energies and relative intensities of the lowest excited states for the triphenylmethyl radical are also largely supported theoretical studies based loosely on Ref. 24, where the first excited state in their results is the 2E state predicted to have a weak absorption at 2.41 eV (515 nm) and their fifth excited state is the 2E state predicted to have an intense absorption at 3.84 eV (322 nm) corresponding to 2^2E in our results.⁹¹ The number of states is different in both methods; however, the energetic ordering of the states captured by both ExROPPP and the method of Ref. 91 is the same. The energies in Ref. 91 were shifted such that the energy of the lowest excited state matched the experimental data, whereas our results are not manipulated in any way to match the experiment.

c. Quartet states. The agreement between the GMC-QDPT and ExROPPP calculated energies for the quartet states is not as good as for the doublet states for the radicals tested. For the allyl radical, the quartet state energy is 6.07 eV in GMC-QDPT and 4.40 eV in ExROPPP. Similarly, for the benzyl radical, GMC-QDPT predicts energies of 4.42 and 5.42 eV for the 1^4B_2 and 1^4A_2 states, respectively, but the ExROPPP values are 3.62 and 4.80 eV, again seeming to underestimate the quartet energy. ExROPPP also seems to largely underestimate the quartet energies for the trityl radical for the 1^4A_2 and 1^4E states when compared to the GMC-QDPT values. In addition, the relative energetic ordering of the doublet and quartet states is different in the GMC-QDPT and ExROPPP results. One possible reason for this discrepancy is that the set of PPP parameters used in this paper (and PPP theory in general) have mainly been applied for calculating the energies of singlet-singlet transitions in closed-shell molecules and, in particular, simulating their spectra, in which only those transitions that are bright are of importance.⁹² Therefore, by analogy, one would expect these parameters to be more accurate for calculating the energies of excited doublet states and less accurate for (dark) excited quartet states in radicals, which is what we observe from our results.

Moreover, it is known to be very difficult to experimentally measure quartet state energies as quartet states are formally dark. In addition, in the case of odd alternant hydrocarbon radicals, the first quartet state is usually higher in energy than the lowest excited doublet state so it is not normally observed through intersystem crossing from the doublet state in the same way that a triplet state is observed via intersystem crossing from the singlet state in a closed-shell molecule.⁹³ As a side note, this is a useful property of such radicals that makes them desirable for making OLEDs, but also

means that the quartet state is rarely observed.^{24,94,95} The experimental quartet energies for the odd alternant hydrocarbon radicals tested, to the best of our knowledge, are absent from the literature, so it is impossible to comment on the accuracy of ExROPPP for quartet states with any certainty.

Finally, on analyzing the CI expansion of the quartet states calculated by ExROPPP, we notice that the quartet states for the trityl, DPXM, PDXM, and TXM radicals have significant contributions from higher excitations ($i > 2$ and $j' > 2'$), and therefore, it is expected that their computed energies will be dependent on the inclusion of such higher excitations.

d. Overall accuracy. Figure 6 shows a comparison of the experimental excitation energies and those computed by using the two theoretical methods. The ExROPPP calculated energies are all close to the experimental values. As mentioned earlier, it is difficult to comment on the accuracy of ExROPPP for the calculation of quartet state energies. The root mean squared (RMS) errors of the ExROPPP and GMC-QDPT results $E_i^{\text{calc.}}$ compared to the experimental excitation energies $E_i^{\text{exp.}}$ have been calculated using the formula,

$$\epsilon_{\text{RMS}} = \sqrt{\frac{1}{N} \sum_{i=1}^N (E_i^{\text{calc.}} - E_i^{\text{exp.}})^2}. \quad (7)$$

The ϵ_{RMS} values for the ExROPPP and GMC-QDPT results are presented in Table IX. It can be seen that ExROPPP calculates excitation energies with a similar accuracy to GMC-QDPT for the doublet

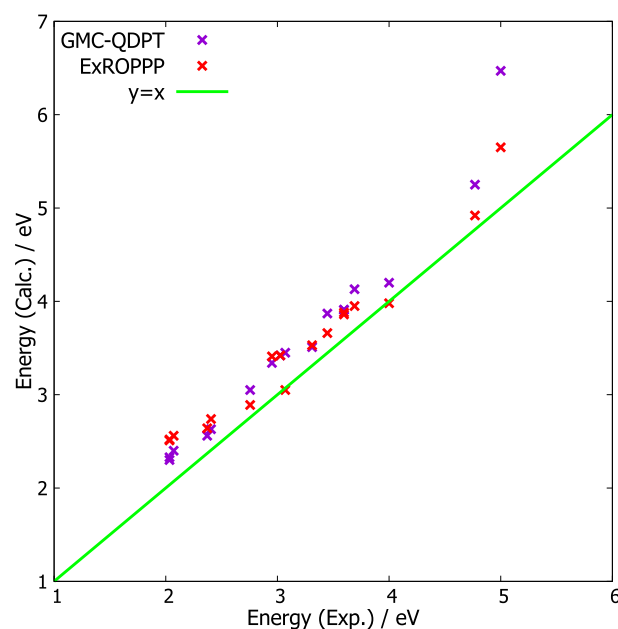


FIG. 6. Comparison of ExROPPP and GMC-QDPT excitation energies to experiment. No results have been shifted to agree with the experiment, and the ExROPPP results are produced using the same parameterization as has previously been used for closed-shell molecules. ExROPPP is found to be as accurate as GMC-QDPT when compared to the experimental energies for doublet states.

TABLE IX. RMS errors of (i) ExROPPP and (ii) GMC-QDPT calculated excited state energies compared to the experimental values and (iii) ExROPPP calculated energies compared to GMC-QDPT for the odd alternant hydrocarbon radicals presented in this paper. The numbers without brackets are for all states, whereas the numbers inside the brackets are calculated for doublet states only.

	$\epsilon_{\text{RMS}}/\text{eV}$
GMC-QDPT vs exp.	(0.48)
ExROPPP vs exp.	(0.33)
ExROPPP vs GMC-QDPT	0.63 (0.50)

states of the alternant hydrocarbon radicals chosen. We must stress that the results of ExROPPP computations presented here are the raw results that are in no way shifted to agree with the experiment (or GMC-QDPT), and the same parameters are used as in previous studies on closed-shell molecules.⁶⁹ Computations using the bases of excitations and of spin-adapted states yield identical results.

In general, the key features of the low lying electronic states of radicals are well captured by using the simple and computationally inexpensive ExROPPP method. For the alternant hydrocarbon radicals studied, the lowest lying electronic state above the ground state is always a doublet D_1 and always has a very weak absorption in the experiment. This state is always $|\Psi_{0i}^- \rangle$ at the ExROPPP level of theory and always in the dark state, but at the higher level of theory in GMC-QDPT, it may have a very small oscillator strength.²⁴ The doublet states $|\Psi_{0i}^+ \rangle$ are always responsible for the low energy intense bands. There are higher lying doublet states of the type $|\Psi_{ij}^+ \rangle$, which are also bright; however, for the molecules tested they lie far into the UV and are of less relevance to the optical properties. Furthermore, it is shown by the ExROPPP calculations that only a small number of excited states, at most $|\Psi_{01}^+ \rangle$, $|\Psi_{02}^+ \rangle$, and $|\Psi_{03}^+ \rangle$, are responsible for the significant features of the UV-visible spectrum for these molecules, involving transitions between the SOMO and the 1, 2, 3, 1', 2, and 3' orbitals.

2. Spin-purity

We calculated $\langle S^2 \rangle_i$ and the degree of spin-contamination $\Delta \langle S^2 \rangle_i$ for each of the ExROPPP states i . We find that $\Delta \langle S^2 \rangle_i = 0$ for all ExROPPP states. However, on the basis of all single excitations only (ROPPP-CIS), $\Delta \langle S^2 \rangle_i \neq 0$ for all states (apart from for the allyl radical, where only some states are contaminated, but this is a special case and not the trend), and $\Delta \langle S^2 \rangle_i$ is generally significantly large, as

presented in Table X. See Sec. V C in the supplementary material for the calculation of spin-contamination.

3. Speed

The speed of the ExROPPP method was compared to that of the accurate post-Hartree-Fock method, GMC-QDPT, for the radicals studied. These results are presented in Table XI. GMC-QDPT calculations on all radicals were performed using GAMESS-US using 2 cores on a desktop computer, and all ExROPPP calculations were performed using Python 3 using the same desktop computer and utilized 8 cores. The timings from ExROPPP presented here are for proof of concept purposes only since the ExROPPP code has not been optimized and was coded in Python; however, it clearly offers a substantial reduction in the computation time compared to GMC-QDPT. We leave optimization of the ExROPPP code and rigorous benchmarking for future work. We defined the speed-up factor as $t_{\text{GMC-QDPT}}/t_{\text{ExROPPP}}$.

B. Alternacy rules

In this section, we apply the algebra of XCIS on the basis of spin-adapted *plus* and *minus* states to alternant hydrocarbon radicals. Using this method, we can deduce simple and widely applicable rules for the interaction of the excited states of alternant hydrocarbon radicals, which may guide spectral interpretation and molecular design of emissive radicals.

It has long been known that due to pseudoparity, the excited states of closed-shell alternant hydrocarbons can be factored into *plus* and *minus* combinations, and that a further set of Hamiltonian interaction and dipole moment selection rules apply to them in addition to the usual rules concerning symmetry and spin.²⁸ These rules were originally derived by Pariser considering the ground state and single-excitations and using the approximations of NDO and zero resonance integrals between the non-nearest-neighbouring atoms. While the idea of pseudoparity has been known for a long time to also apply to radicals,²⁴ and some of Pariser's rules have been explored in special cases; to the best of our knowledge, there has yet to be an attempt to derive a general set of rules for alternant hydrocarbon radicals. In this section, we test Pariser's rules to see if they also apply to radicals. We apply the equations for the XCIS method for the radicals mentioned above to derive the Hamiltonian and dipole moment interaction elements of *plus* and *minus* states, as it is the analog for radicals of CIS in closed-shell systems.

TABLE X. Demonstration of spin-contamination $\Delta \langle S^2 \rangle$, resulting from the use of a basis of all single-excitations. The excited states calculated by (a) ROPPP-CIS (CIS with restricted open-shell PPP reference with all single excitations) and (b) ExROPPP for the benzyl radical (C_{2v} point group) are presented and compared to the results of the GMC-QDPT calculations and experimental data.⁸⁶ $1B_2$ is the ground state.

State	$\langle S^2 \rangle_a$	$\langle S^2 \rangle_b$	$\Delta \langle S^2 \rangle_a$	$\Delta \langle S^2 \rangle_b$	E_a (eV)	E_b (eV)	$E_{\text{GMC-QDPT}}$ (eV)	$E_{\text{exp.}}$ (eV)
$1B_2$	0.789	0.75	0.276	0	n/a	n/a	n/a	n/a
$1A_2$	1.016	0.75	0.679	0	2.99	2.89	3.05	2.76
$2A_2$	0.866	0.75	0.467	0	3.96	3.98	4.20	4.00
$4B_2$	0.761	0.75	0.146	0	4.83	4.92	5.25	4.77

TABLE XI. Comparison of the speed of the ExROPPP method with GMC-QDPT. The GMC-QDPT calculations are for doublet calculations only and are at least two orders of magnitude slower than ExROPPP. The timings given are the total CPU time.

Molecule	$t_{\text{GMC-QDPT/s}}$	$t_{\text{ExROPPP/s}}$	Speed-up factor
Allyl	9.26	0.0231	402
Benzyl	1560	0.157	9970
DPM	22 000	0.511	43 000
Trityl	8670	1.58	5500
DPXM	31 800	4.10	7740
PDXM	80 800	8.74	9250
TXM	163 000	18.1	9020

In order to get a complete picture of the interaction of the excited states of radicals, we need to consider the *plus* and *minus* combinations of all XCIS states. The *plus* and *minus* states with one open-shell have already been worked out for us by Longuet-Higgins and Pople and are given in Sec. II Eq. (6).²⁴ However, as far as we are aware, Longuet-Higgins and Pople did not consider the pseudoparity adapted states of three open-shells and we must now define them. The doublet and quartet states with three open-shells also come in degenerate pairs, and we can make the following linear combinations of these pairs of states:

$$|^{2S}\Psi_{ij}^{\pm}\rangle = \frac{1}{\sqrt{2}}(|^{2S}\Psi_i^{\prime\prime}\rangle \pm |^{2S}\Psi_j^{\prime\prime}\rangle), \quad (8a)$$

$$|^{2T}\Psi_{ij}^{\pm}\rangle = \frac{1}{\sqrt{2}}(|^{2T}\Psi_i^{\prime\prime}\rangle \mp |^{2T}\Psi_j^{\prime\prime}\rangle), \quad (8b)$$

$$|^4\Psi_{ij}^{\pm}\rangle = \frac{1}{\sqrt{2}}(|^4\Psi_i^{\prime\prime}\rangle \pm |^4\Psi_j^{\prime\prime}\rangle), \quad (8c)$$

where $i \neq j$. When $i = j$, Eqs. (8a)–(8c) are no longer valid and only one state $|^X\Psi_i^{\prime\prime}\rangle$ exists (where $X = 2S, 2T$, or 4). Note that we have defined the $|^{2T}\Psi_{ij}^{\pm}\rangle$ linear combinations with the opposite signs to the other two pairs of states, i.e., for $|^{2S}\Psi_{ij}^{\pm}\rangle$ and $|^4\Psi_{ij}^{\pm}\rangle$, the *plus* state has a “+” sign and the *minus* state has a “−” sign in their expansions in Eq. (8a) and Eq. (8c), respectively. However, for $|^{2T}\Psi_{ij}^{\pm}\rangle$, the *plus* state has a “−” sign and the *minus* state has a “+” sign. The reason for this seemingly inconsistent definition will become apparent when we make the approximations relating to alternant hydrocarbons.

Now that we have defined a complete basis of pseudoparity and spin-adapted states, we can derive the exact matrix elements for the XCIS Hamiltonian $\mathbf{H}_{\text{XCIS}}^{\text{p}}$ on this basis, using the equations presented in Tables IX and X in the supplementary material, Sec. IV as discussed above. These are presented in the supplementary material, Sec. IV C in Table XI. We also derive the exact dipole moments $\mathbf{M}_{\text{XCIS}}^{\text{p}}$ on the basis of *plus* and *minus* states, which are presented in Table XV in the supplementary material, Sec. VI G.

We then consider the effect of the same approximations as Pariser did on the XCIS Hamiltonian and dipole moments, in addition to the assumption that the Fock matrix is diagonalized,

i.e., $F_{ij} = \delta_{ij}\epsilon_i$ (in other words, this requires that the orbitals used in forming the Hamiltonian are the converged molecular orbitals). After making this series of approximations, the matrix elements simplify greatly and many of which vanish. The XCIS Hamiltonian $\mathbf{H}_{\text{XCIS}}^{\text{a}}$ and dipole moment operator $\mathbf{M}_{\text{XCIS}}^{\text{a}}$ on the basis of pseudoparity and spin-adapted states under the aforementioned approximations are given in Tables XI and XV, respectively, in Secs. II D and II H of the supplementary material. From this algebra, clear rules for the excited state spectra of alternant radical hydrocarbons emerge, which are similar but not identical to those for closed-shell molecules and which can be found in Table XII.

First, we find that there is zero Hamiltonian interaction between the *plus* and *minus* states of alternant hydrocarbon radicals. This has been previously shown to be true for closed-shell alternant hydrocarbons.²⁸ In the case of radicals although there is the aforementioned caveat that we have to define the $|^{2T}\Psi_{ij}^{\pm}\rangle$ states with the opposite signs in their expansion in terms of $|^{2T}\Psi_i^{\prime\prime}\rangle$ and $|^{2T}\Psi_j^{\prime\prime}\rangle$, and additionally, we notice that the $|^{2T}\Psi_i^{\prime\prime}\rangle$ states behave as *minus* states, whereas $|^{2S}\Psi_i^{\prime\prime}\rangle$ and $|^4\Psi_i^{\prime\prime}\rangle$ behave as *plus* states. We find that for radicals, the ground state behaves like a *minus* state and only interacts with other *minus* states. In closed-shell alternant hydrocarbons, this is also true; however, due to Brillouin’s theorem only higher than singly excited *minus* states may interact with the ground state. On the other hand, a weaker version of Brillouin’s theorem applies for radicals where singly excited states of the type $|^2\Psi_{0i}^{\pm}\rangle$ may mix with the ground state but all other purely singly excited states are forbidden from interacting with the ground state ($|^{2T}\Psi_i^{\prime\prime}\rangle$ and $|^{2T}\Psi_{ij}^{\pm}\rangle$ interact with $|^2\Psi_0\rangle$ but have doubly excited character). The Hamiltonian interaction rules for radicals are shown pictorially below in Fig. 7 and presented algebraically in Table XII in the supplementary material, Sec. IV D.

Furthermore, Pariser showed that for closed-shell molecules, the Hamiltonian on the basis of singlet *minus* states $|^1\Psi_{ij}^{\pm}\rangle$ is exactly the same as the Hamiltonian on the basis of triplet *minus* states $|^3\Psi_{ij}^{\pm}\rangle$. While this is an interesting observation, we find no corresponding rule for radicals: no two non-zero Hamiltonian matrix elements are in general the same.

Second, we find that for radicals, the dipole moments between two *plus* states or between two *minus* states are exactly zero. This selection rule applies on top of the more general spin selection rule and any selection rules imposed by point group symmetry.^{34,96} This pseudoparity selection rule has been previously known for closed-shell alternant hydrocarbons.²⁸ Consequently, the transition dipole moment between two states may be non-zero if and only if the states are of opposite pseudoparity and equal multiplicity and regardless of whether the alternant hydrocarbon is closed-shell or a radical. It follows that the ground-state and any XCIS states of an alternant hydrocarbon have a zero permanent dipole moment. The pseudoparity selection rule for radicals is shown pictorially in Fig. 8 and presented algebraically in Table XVI in the supplementary material, Sec. IV H.

All of the above-mentioned rules hold even after configuration interaction. That is, there exist four sets of states grouped by pseudoparity (*plus* or *minus*) and multiplicity (singlet/doublet or triplet/quartet), where any member of one set does not interact

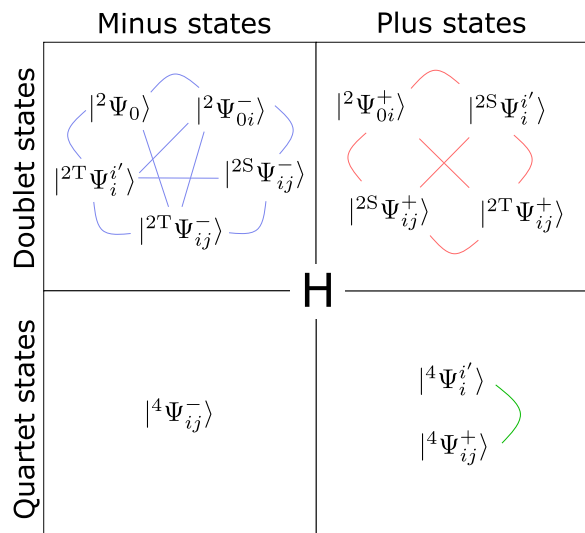


FIG. 7. Interaction of the electronic excited states of an alternant hydrocarbon radical via the Hamiltonian \hat{H} . The lines drawn between the states represent an interaction via \hat{H} . The states may interact if and only if they are in the same quadrant.

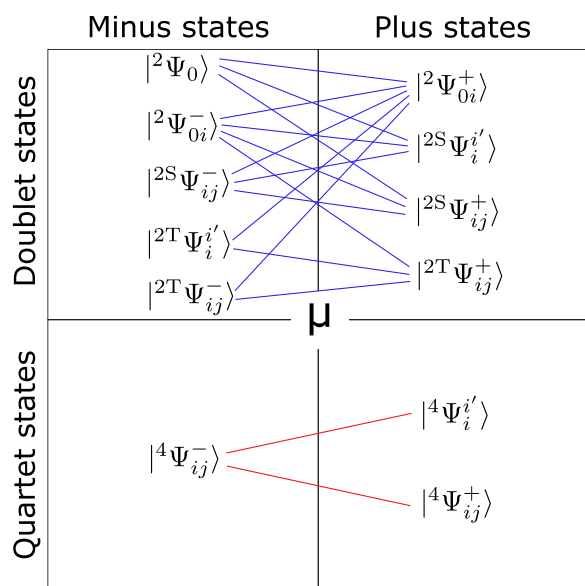


FIG. 8. Interaction of the electronic excited states of an alternant hydrocarbon radical via the dipole moment operator $\hat{\mu}$. The lines drawn between the states represent an interaction via $\hat{\mu}$. Only states with the same multiplicity and opposite pseudoparity may interact through the dipole moment operator.

via the Hamiltonian with any member of any other set before and after configuration interaction. Furthermore, states of the same pseudoparity and/or opposite multiplicity have zero dipole moments between one another before and after configuration interaction.

Specifically concerning their dipole moment from the ground state $|\Psi_0\rangle$ (which is a *minus* state of the lowest multiplicity), *plus* states of the same multiplicity may be bright and have a non-zero transition dipole moment, whereas *minus* states are always dark, even after configuration interaction. However, there are cases where *plus* states of the same multiplicity as the ground state may be completely dark (such as $|\Psi_{ij}^+\rangle$) or may have vanishingly small transition dipole moments; however, this is not in violation of any of the above-mentioned rules. As a result of the dipole pseudoparity selection rule for alternant hydrocarbons and it holding after configuration interaction, it is usually (but *not* always) the case that the lowest energy electronic excited state of an alternant hydrocarbon radical is completely dark at this level of theory^{91,97} and is expected to have a vanishingly small dipole moment in the experiment and in calculations at higher levels of theory.^{85–87,90,98–100} The reason for this is that the lowest state is usually a doublet *minus* state of the form $|\Psi_{i0}^-\rangle$.^{24,101} The lowest excited state cannot be $|\Psi_{i0}^+\rangle$ as there will always be a corresponding *minus* state of lower energy.^{24,101} If the first excited state is not $|\Psi_{i0}^-\rangle$ then it must contain at least some contribution from configurations of three open-shells. Inspecting the relevant matrix elements in the supplementary material, Table XII, we find that $|\Psi_{ij}^+\rangle$ is always the lowest energy configuration out of all of those with open-shells in i , 0 , and j' , and $|\Psi_i^+\rangle$ is always the lowest energy configuration out of all of those with open-shells in i , 0 , and i' , so it is likely but not certain that in the case that $|\Psi_{i0}^-\rangle$ is not lowest in energy, the lowest energy state will be a quartet state, which will also be dark.

For practical purposes, the alternancy rules presented here mean that the UV–vis spectrum of an alternant hydrocarbon radical will show a very weak absorption at low energies (corresponding to D_1 that will usually be $|\Psi_{10}^-\rangle$) and an intense absorption at higher energies (usually corresponding to $|\Psi_{10}^+\rangle$). Since emission is usually from the lowest excited state according to Kasha's rule, emission from alternant radicals is likely to be slow and outcompeted by non-radiative decay. Consequently, organic radicals for OLEDs should not be alternant hydrocarbons. These rules are consistent with, but stronger than, the previous design rules that emissive radicals should be non-alternant.^{27,100} It was previously known that D_1 would usually be $|\Psi_{10}^-\rangle$ and dark, but this did not exclude the possibility of $|\Psi_{10}^-\rangle$ mixing with, and borrowing intensity¹⁰² from, higher-lying bright excitations. However, the alternancy rules derived here show that $|\Psi_{10}^-\rangle$ can mix only with other *minus* excitations, which also have zero dipole moments with the ground state, such that after configuration interaction, $|\Psi_{10}^-\rangle$ will remain dark.

In addition, although the alternancy rules derived here, strictly speaking, only hold for purely hydrocarbon radicals, they are likely to hold qualitatively for chlorinated radicals, such as the tris-(2,4,6-trichlorophenyl)-methyl (TTM) and perchlorotriphenyl-methyl (PTM) radicals, where the high electronegativity of chlorine compared to carbon and the mismatch between its 3p orbitals and the 2p orbitals of carbon mean that it is unlikely to participate significantly in the electronic structure in the conjugated system.^{100,101}

Comparing the above-mentioned alternancy rules with the numerical results from ExROPPP calculations on alternant hydrocarbons presented in Sec. IV A, we see that the results of ExROPPP are entirely consistent with these rules. This is presented in

TABLE XII. Novel excited state interaction rules derived for alternant hydrocarbon radicals compared to those already existing for closed-shell alternant hydrocarbons.

Rule	Radical	Closed-shell
1	All states belong to one of two pseudoparity groups, <i>plus</i> or <i>minus</i> .	All states belong to one of two pseudoparity groups, <i>plus</i> or <i>minus</i> .
2	Degeneracy: $E(^2\Psi_i^0) = E(^2\Psi_0')$ $E(^{2S}\Psi_i^j) = E(^{2S}\Psi_j')$ $E(^{2T}\Psi_i^j) = E(^{2T}\Psi_j')$ $E(^4\Psi_i^j) = E(^4\Psi_j')$	Degeneracy: $E(^1\Psi_i^j) = E(^1\Psi_j')$ $E(^3\Psi_i^j) = E(^3\Psi_j')$
3	<i>Plus</i> and <i>minus</i> states: $ \Psi_{0i}^\pm\rangle = \frac{1}{\sqrt{2}}(^2\Psi_i^0\rangle \pm ^2\Psi_0'\rangle)$ $ \Psi_{ij}^{2S}\rangle = \frac{1}{\sqrt{2}}(^{2S}\Psi_i^j\rangle \pm ^{2S}\Psi_j'\rangle)$ $ \Psi_{ij}^{2T}\rangle = \frac{1}{\sqrt{2}}(^{2T}\Psi_i^j\rangle \mp ^{2T}\Psi_j'\rangle)$ $ \Psi_{ij}^4\rangle = \frac{1}{\sqrt{2}}(^4\Psi_i^j\rangle \pm ^4\Psi_j'\rangle)$ $ \Psi_i^{2S}\rangle$ and $ \Psi_i^4\rangle$ are <i>plus</i> states but $ \Psi_i^{2T}\rangle$ is a <i>minus</i> state. $ \Psi_0^2\rangle$ is a <i>minus</i> state.	<i>Plus</i> and <i>minus</i> states: $ \Psi_i^{1,\pm}\rangle = \frac{1}{\sqrt{2}}(^1\Psi_i^j\rangle \pm ^1\Psi_j'\rangle)$ $ \Psi_i^{3,\pm}\rangle = \frac{1}{\sqrt{2}}(^3\Psi_i^j\rangle \pm ^3\Psi_j'\rangle)$ $ \Psi_i^1\rangle$ and $ \Psi_i^3\rangle$ are <i>plus</i> states. $ \Psi_0^1\rangle$ is a <i>minus</i> state.
4		
5	There is zero Hamiltonian interaction between <i>plus</i> and <i>minus</i> states.	There is zero Hamiltonian interaction between <i>plus</i> and <i>minus</i> states.
6	N/A	$\langle^1\Psi_{ij}^- \hat{H} ^1\Psi_{kl}^- \rangle = \langle^3\Psi_{ij}^- \hat{H} ^3\Psi_{kl}^- \rangle$
7	For any two arbitrary states $ \Psi_u\rangle$ and $ \Psi_v\rangle$, $\langle\Psi_u \hat{\mu} \Psi_v\rangle$ may be non-zero if and only if $ \Psi_u\rangle$ and $ \Psi_v\rangle$ have equal multiplicity and opposite pseudoparity.	For any two arbitrary states $ \Psi_u\rangle$ and $ \Psi_v\rangle$, $\langle\Psi_u \hat{\mu} \Psi_v\rangle$ may be non-zero if and only if $ \Psi_u\rangle$ and $ \Psi_v\rangle$ have equal multiplicity and opposite pseudoparity.
8	D_1 state usually $ \Psi_{01}^- \rangle$, which is always dark.	S_1 state usually $ \Psi_1^1 \rangle$, which is usually bright.
9	$E(^2\Psi_{0i}^+) - E(^2\Psi_{0i}^-) = 2K_{i0} \geq 0$	N/A
10	Rules 1, 5, and 7 hold after configuration interaction.	Rules 1, 5, and 7 hold after configuration interaction.

Tables I–VII in Sec. I of the supplementary material, where the energies, oscillator strengths, and CI expansion coefficients of the ExROPPP states are tabulated.

V. CONCLUSIONS

In this article, we have combined previous ideas that adding certain double excitations to a radical CIS calculation can lead to spin purity^{24,25,27} with Pariser–Parr–Pople theory^{28,70–73} to obtain a computational method for the low-lying electronically excited states of hydrocarbon radicals. This method, which we call ExROPPP, reproduces experimental doublet excitation energies and intensities for a series of odd alternant hydrocarbon radicals accurately and with minimal computational effort, with a similar degree of accuracy to the general multiconfigurational quasi-degenerate perturbation theory (GMC-QDPT), an accurate multiconfigurational SCF method. In addition, using the approximations of PPP theory, we have derived widely applicable rules for alternant hydrocarbons,

which should aid in the prediction, assignment, and interpretation of their spectra.

There are many avenues for future research. The proof-of-concept calculations in this paper are for hydrocarbon radicals (for which, there already exists tested parameterization), and we plan to extend this method to radicals containing nitrogen and chlorine, such as the breakthrough fluorescent radical TTM-3NCz,³ sulfur containing radicals, such as those based on thiophene,⁷ and non-alternant and ionic radicals. There are possibilities of using machine learning¹⁰³ to optimize ExROPPP parameterization, especially for heteroatoms and for quartet states, given that our initial results suggest that ExROPPP is less accurate for quartet state energies than doublet state energies. The ExROPPP method could be extended to radicals with more than one unpaired electron in their ground state,²² and the alternacy rules that we have derived for monoradicals may be extendable to these systems. It is our hope that ExROPPP can be extended to accurately and quickly simulate a wide range of conjugated organic radicals, becoming a useful tool for rapid spectral determination. This can then be used to design highly efficient and

emissive radicals²⁷ for applications such as OLEDs³ and quantum computing.²¹

SUPPLEMENTARY MATERIAL

The supplementary material contains tables presenting detailed energies, oscillator strengths/intensities, and composition of excited states calculated by ExROPPP and GMC-QDPT and obtained from experimental data. It also contains molecular geometries used for the calculations and any other details of the computational methods used in this paper.

ACKNOWLEDGMENTS

The authors thank Emrys W. Evans for helpful suggestions on the research. TJHH acknowledges the Royal Society University Research Fellowship Grant No. URF\R1\201502 and the startup grant from University College London.

AUTHOR DECLARATIONS

Conflict of Interest

The authors have no conflicts to disclose.

Author Contributions

James D. Green: Conceptualization (supporting); Data curation (lead); Formal analysis (lead); Investigation (lead); Methodology (lead); Project administration (lead); Software (lead); Writing – original draft (lead); Writing – review & editing (equal). **Timothy J. H. Hele:** Conceptualization (lead); Funding acquisition (lead); Investigation (supporting); Methodology (supporting); Project administration (supporting); Supervision (lead); Writing – original draft (supporting); Writing – review & editing (equal).

DATA AVAILABILITY

The data that support the findings of this study are available within the article and its supplementary material.

REFERENCES

- H. Hiratsuka, S. Rajadurai, P. K. Das, G. L. Hug, and R. W. Fessenden, *Chem. Phys. Lett.* **137**, 255 (1987).
- Q. Peng, A. Obolda, M. Zhang, and F. Li, *Angew. Chem., Int. Ed.* **54**, 7091 (2015).
- X. Ai, E. W. Evans, S. Dong, A. J. Gillett, H. Guo, Y. Chen, T. J. H. Hele, R. H. Friend, and F. Li, *Nature* **563**, 536 (2018).
- H. Guo, Q. Peng, X.-K. Chen, Q. Gu, S. Dong, E. W. Evans, A. J. Gillett, X. Ai, M. Zhang, D. Credgington *et al.*, *Nat. Mater.* **18**, 977 (2019).
- Z. Cui, A. Abdurahman, X. Ai, and F. Li, *CCS Chem.* **2**, 1129 (2020).
- F. Li, A. J. Gillett, Q. Gu, J. Ding, Z. Chen, T. J. H. Hele, W. K. Myers, R. H. Friend, and E. W. Evans, *Nat. Commun.* **13**, 2744 (2022).
- P. Murto, R. Chowdhury, S. Gorgon, E. Guo, W. Zeng, B. Li, Y. Sun, H. Francis, R. H. Friend, and H. Bronstein, *Nat. Commun.* **14**, 4147 (2023).
- H.-H. Cho, S. Gorgon, G. Londi, S. Giannini, C. Cho, P. Ghosh, C. Tonnelé, D. Casanova, Y. Olivier, F. Li, D. Beljonne, N. Greenham, R. Friend, and E. Evans, “Efficient near-infrared organic light-emitting diodes with emission from spin doublet excitons,” [arXiv:2308.02355](https://arxiv.org/abs/2308.02355) (2023).

- M. A. Baldo, D. F. O'Brien, Y. You, A. Shoustikov, S. Sibley, M. E. Thompson, and S. R. Forrest, *Nature* **395**, 151 (1998).
- M. A. Baldo, D. F. O'Brien, M. E. Thompson, and S. R. Forrest, *Phys. Rev. B* **60**, 14422 (1999).
- R. H. Friend, R. Gymer, A. Holmes, J. Burroughes, R. Marks, C. Taliani, D. Bradley, D. A. D. Santos, J.-L. Bredas, M. Lögdlund, and W. R. Salaneck, *Nature* **397**, 121 (1999).
- J. Wang, A. Chepelianskii, F. Gao, and N. C. Greenham, *Nat. Commun.* **3**, 1191 (2012).
- B. Minaev, G. Baryshnikov, and H. Agren, *Phys. Chem. Chem. Phys.* **16**, 1719 (2014).
- S.-J. Su, T. Chiba, T. Takeda, and J. Kido, *Adv. Mater.* **20**, 2125 (2008).
- V. Jankus, P. Data, D. Graves, C. McGuinness, J. Santos, M. R. Bryce, F. B. Dias, and A. P. Monkman, *Adv. Funct. Mater.* **24**, 6178 (2014).
- Z. Guo, S. Park, J. Yoon, and I. Shin, *Chem. Soc. Rev.* **43**, 16 (2014).
- M. Blanco and I. Villarroya, *TrAC, Trends Anal. Chem.* **21**, 240 (2002).
- A. Sakudo, *Clin. Chim. Acta* **455**, 181 (2016).
- V. R. Kondepati, H. M. Heise, and J. Backhaus, *Anal. Bioanal. Chem.* **390**, 125 (2008).
- J. Clark and G. Lanzani, *Nat. Photonics* **4**, 438 (2010).
- S. Gorgon, K. Lv, J. Grüne, B. H. Drummond, W. K. Myers, G. Londi, G. Ricci, D. Valverde, C. Tonnelé, P. Murto, A. S. Romanov, D. Casanova, V. Dyakonov, A. Sperlich, D. Beljonne, Y. Olivier, F. Li, R. H. Friend, and E. W. Evans, *Nature* **620**, 538 (2023).
- T. Stuyver, B. Chen, T. Zeng, P. Geerlings, F. De Proft, and R. Hoffmann, *Chem. Rev.* **119**, 11291 (2019).
- H. C. Longuet-Higgins, *J. Chem. Phys.* **18**, 265 (1950).
- H. C. Longuet-Higgins and J. A. Pople, *Proc. Phys. Soc., Sect. A* **68**, 591 (1955).
- D. Maurice and M. Head-Gordon, *J. Phys. Chem.* **100**, 6131 (1996).
- M. Roemelt and F. Neese, *J. Phys. Chem. A* **117**, 3069 (2013).
- T. J. H. Hele, *Physical Chemistry of Semiconductor Materials and Interfaces XX* (International Society for Optics and Photonics, SPIE, 2021), Vol. 11799, p. 117991A.
- R. Pariser, *J. Chem. Phys.* **24**, 250 (1956).
- J. A. Pople and R. K. Nesbet, *J. Chem. Phys.* **22**, 571 (1954).
- C. C. J. Roothaan, *Rev. Mod. Phys.* **32**, 179 (1960).
- S. Huzinaga, *Phys. Rev.* **122**, 131 (1961).
- E. R. Davidson, *Chem. Phys. Lett.* **21**, 565 (1973).
- J. Binkley, J. Pople, and P. Dobosh, *Mol. Phys.* **28**, 1423 (1974).
- A. Szabo and N. Ostlund, “Modern quantum Chemistry: Introduction to advanced electronic structure theory,” *Dover Books on Chemistry* (Dover Publications, 1989).
- V. Barone, C. Adamo, and N. Russo, *Chem. Phys. Lett.* **212**, 5 (1993).
- O. L. Malkina, J. Vaara, B. Schimmelpennig, M. Munzarová, V. G. Malkin, and M. Kaupp, *J. Am. Chem. Soc.* **122**, 9206 (2000).
- F. Rastrelli and A. Bagno, *Chem. - Eur. J.* **15**, 7990 (2009).
- R. Caballol, O. Castell, F. Illas, I. de P R Moreira, and J. P. Malrieu, *J. Phys. Chem. A* **101**, 7860 (1997).
- F. Neese, *Coord. Chem. Rev.* **253**, 526 (2009), part of Special Issue: Theory and Computing in Contemporary Coordination Chemistry.
- P. H. Mueller, N. G. Rondan, K. N. Houk, J. F. Harrison, D. Hooper, B. H. Willen, and J. F. Liebman, *J. Am. Chem. Soc.* **103**, 5049 (1981).
- B. O. Roos, R. Lindh, P. Å. Malmqvist, V. Veryazov, and P.-O. Widmark, *Hartree-Fock Theory* (John Wiley & Sons, Ltd., 2016), Chap. 4, pp. 43–58.
- J. Baker, A. Scheiner, and J. Andzelm, *Chem. Phys. Lett.* **216**, 380 (1993).
- Computational Photochemistry*, edited by M. Merchán, L. Serrano-Andrés, and M. Olivucci, volume 16 of *Theoretical and Computational Chemistry* (Elsevier, 2005), pp. 35–91.
- A. Ipatov, F. Cordova, L. J. Doriol, and M. E. Casida, “Excited-state spin-contamination in time-dependent density-functional theory for molecules with open-shell ground states,” *J. Mol. Struct.: THEOCHEM* **914**, 60 (2009).
- Z. Li and W. Liu, *J. Chem. Phys.* **135**, 194106 (2011).
- K. R. Glaesemann and M. W. Schmidt, *J. Phys. Chem. A* **114**, 8772 (2010).
- T. Tsuchimochi and G. E. Scuseria, *J. Chem. Phys.* **133**, 141102 (2010).

- ⁴⁸P. Kimber and F. Plasser, *Phys. Chem. Chem. Phys.* **22**, 6058 (2020).
- ⁴⁹D. Maurice and M. Head-Gordon, *Int. J. Quantum Chem.* **56**, 361 (1995).
- ⁵⁰H. Werner and W. Meyer, *J. Chem. Phys.* **74**, 5794 (1981).
- ⁵¹P. Å. Malmqvist and B. O. Roos, *Chem. Phys. Lett.* **155**, 189 (1989).
- ⁵²H. Nakano, *J. Chem. Phys.* **99**, 7983 (1993).
- ⁵³A. Marie and H. G. A. Burton, *J. Phys. Chem. A* **127**, 4538 (2023).
- ⁵⁴J. Ivanic, *J. Chem. Phys.* **119**, 9364 (2003).
- ⁵⁵B. R. Brooks and H. F. Schaefer III, *J. Chem. Phys.* **70**, 5092 (1979).
- ⁵⁶P. G. Szalay and J. Gauss, *J. Chem. Phys.* **112**, 4027 (2000).
- ⁵⁷M. Schreiber, M. R. Silva-Junior, S. P. A. Sauer, and W. Thiel, *J. Chem. Phys.* **128**, 134110 (2008).
- ⁵⁸T. J. H. Hele, B. Monserrat, and A. M. Alvertis, *J. Chem. Phys.* **154**, 244109 (2021).
- ⁵⁹G. H. Booth and A. Alavi, *J. Chem. Phys.* **132**, 174104 (2010).
- ⁶⁰R. E. Thomas, Q. Sun, A. Alavi, and G. H. Booth, *J. Chem. Theory Comput.* **11**, 5316 (2015).
- ⁶¹M. R. Silva-Junior, M. Schreiber, S. P. A. Sauer, and W. Thiel, *J. Chem. Phys.* **129**, 104103 (2008).
- ⁶²A. D. Laurent and D. Jacquemin, *Int. J. Quantum Chem.* **113**, 2019 (2013).
- ⁶³A. Dreuw, J. L. Weisman, and M. Head-Gordon, *J. Chem. Phys.* **119**, 2943 (2003).
- ⁶⁴M. J. G. Peach, P. Benfield, T. Helgaker, and D. J. Tozer, *J. Chem. Phys.* **128**, 044118 (2008).
- ⁶⁵T. Stein, L. Kronik, and R. Baer, *J. Chem. Phys.* **131**, 244119 (2009).
- ⁶⁶M. Alipour and Z. Safari, *Phys. Chem. Chem. Phys.* **22**, 27060 (2020).
- ⁶⁷R. Gómez-Bombarelli, J. Aguilera-Iparraguirre, T. D. Hirzel, D. Duvenaud, D. Maclaurin, M. A. Blood-Forsythe, H. S. Chae, M. Einzinger, D.-G. Ha, T. Wu *et al.*, *Nat. Mater.* **15**, 1120 (2016).
- ⁶⁸Z. Yu, Q. Li, Q. Ma, W. Ye, Z. An, and H. Ma, *Chem. Mater.* **35**, 1827 (2023).
- ⁶⁹J. D. Green, E. G. Fuemmeler, and T. J. H. Hele, *J. Chem. Phys.* **156**, 180901 (2022).
- ⁷⁰R. Pariser and R. G. Parr, *J. Chem. Phys.* **21**, 466 (1953).
- ⁷¹J. A. Pople, *Trans. Faraday Soc.* **49**, 1375 (1953).
- ⁷²J. A. Pople, *Proc. Phys. Soc., Sect. A* **68**, 81 (1955).
- ⁷³J. Koutecký, *Chem. Phys. Lett.* **1**, 249 (1967).
- ⁷⁴C. A. Coulson and G. S. Rushbrooke, *Math. Proc. Cambridge Philos. Soc.* **36**, 193–200 (1940).
- ⁷⁵C. He, Z. Li, Y. Lei, W. Zou, and B. Suo, *J. Phys. Chem. Lett.* **10**, 574 (2019).
- ⁷⁶T. J. H. Hele, E. G. Fuemmeler, S. N. Sanders, E. Kumarasamy, M. Y. Sfeir, L. M. Campos, and N. Ananth, *J. Phys. Chem. A* **123**, 2527 (2019).
- ⁷⁷A. M. Alvertis, S. Lukman, T. J. H. Hele, E. G. Fuemmeler, J. Feng, J. Wu, N. C. Greenham, A. W. Chin, and A. J. Musser, *J. Am. Chem. Soc.* **141**, 17558 (2019).
- ⁷⁸M. J. S. Dewar, J. A. Hashmall, and C. G. Venier, *J. Am. Chem. Soc.* **90**, 1953 (1968).
- ⁷⁹P. R. Callis, T. W. Scott, and A. C. Albrecht, *J. Chem. Phys.* **78**, 16 (1983).
- ⁸⁰T. P. Živković, *Int. J. Quantum Chem.* **34**, 333 (1988).
- ⁸¹S. Karabunarliev and N. Tyutyulkov, *Theor. Chim. Acta* **76**, 65 (1989).
- ⁸²T. Schultz, J. S. Clarke, T. Gilbert, H.-J. Deyerl, and I. Fischer, *Faraday Discuss.* **115**, 17 (2000).
- ⁸³K. Tonokura and M. Koshi, *J. Phys. Chem. A* **104**, 8456 (2000).
- ⁸⁴C. L. Currie and D. A. Ramsay, *J. Chem. Phys.* **45**, 488 (1966).
- ⁸⁵D. C. Waterman and M. Dole, *J. Phys. Chem.* **74**, 1906 (1970).
- ⁸⁶P. M. Johnson and A. C. Albrecht, *J. Chem. Phys.* **48**, 851 (1968).
- ⁸⁷A. Bromberg and D. Meisel, *J. Phys. Chem.* **89**, 2507 (1985).
- ⁸⁸W. Bingel, *Z. Naturforsch. A* **10**, 462 (1955).
- ⁸⁹Y. A. Kruglyak and E. Mozdor, *Theor. Chim. Acta* **15**, 374 (1969).
- ⁹⁰T. Li Chu and S. I. Weissman, *J. Chem. Phys.* **22**, 21 (1954).
- ⁹¹J. N. Murrell, *J. Chem. Phys.* **26**, 1738 (1957).
- ⁹²N. Mataga and K. Nishimoto, *Z. Phys. Chem.* **13**, 140 (1957).
- ⁹³J. Shaikh, D. G. Congrave, A. Forster, A. Minotto, F. Cacialli, T. J. H. Hele, T. J. Penfold, H. Bronstein, and T. M. Clarke, *Chem. Sci.* **12**, 8165 (2021).
- ⁹⁴F. Bayrakceken and J. E. Nicholas, *J. Chem. Soc. B* **1970**, 691.
- ⁹⁵M. Fukushima and K. Obi, *J. Chem. Phys.* **93**, 8488 (1990).
- ⁹⁶P. W. Atkins and R. S. Friedman, *Molecular Quantum Mechanics* (Oxford University Press, 2011).
- ⁹⁷Y. Mori, *Bull. Chem. Soc. Jpn.* **34**, 1031 (1961).
- ⁹⁸R. L. McCarthy and A. MacLachlan, *Trans. Faraday Soc.* **56**, 1187 (1960).
- ⁹⁹B. R. Arnold and J. Scaiano, *Macromolecules* **25**, 1582 (1992).
- ¹⁰⁰A. Abdurahman, T. J. Hele, Q. Gu, J. Zhang, Q. Peng, M. Zhang, R. H. Friend, F. Li, and E. W. Evans, *Nat. Mater.* **19**, 1224 (2020).
- ¹⁰¹J. M. Hudson, T. J. H. Hele, and E. W. Evans, *J. Appl. Phys.* **129**, 180901 (2021).
- ¹⁰²G. W. Robinson, *J. Chem. Phys.* **46**, 572 (1967).
- ¹⁰³P. O. Dral and M. Barbatti, *Nat. Rev. Chem* **5**, 388 (2021).